PROCEEDINGS, Twenty-Seventh Workshop on Geothermal Reservoir Engineering
Stanford University, Stanford, California, January 28-30, 2002
SGP-TR-171

A NOVEL WAY TO IDENTIFY FRACTURE AND RESERVOIR CHARACTERISTICS BY FIBER-OPTIC DISTRIBUTED TEMPERATURE LOG

Naotsugu IKEDA

Shincoh Co.
Minami-Tenjin Bldg.8f Watanabe-Dori 5-14-12, Chuo-Ku,
Fukuoka, Fukuoka, 810-0004, Japan
e-mail:ikeda_naotsugu@shincoh.co.jp

ABSTRACT

For wells where the welbore fluid is brine and the plug flow regime is assumed, the wellbore fluid in a given section should retain its enthalpy for certain duration when it moves along the borehole. If fluid is not lost out of hole, the temperature profile shall move together with the fluid until its feature eventually disappears. In other words, by analyzing movement of the temperature profile, one can derive flow profile in the wellbore.

For old field such as Hacchobaru-Otake in Japan, where the long term production and re-injection may have distorted the hydrological system, cross-flows between the permeable planes occur once the borehole penetrates through them. Water is injected to the well whilst observing transient temperature profiles by Fiber-Optic Distributed Temperature Log which then renders a fluid flow profile for the corresponding hydrostatic column. Once the water injection is stopped, the water level goes back to the original. So does the cross-flow profile. However, since the temperature profile is distorted from the one under the original steady state, the cross-flow profile can be observed by the transient temperature phenomena. Furthermore hydrostatic pressure computed by the water column is valid even for dynamic conditions since the temperature profile is instantly acquired.

Now two sets of the fluid flow profiles for the hydrostatic pressures are available, which then render two sets of plot on pressure vs. flowrate. From these plots, one can derive intrinsic pore pressure and a kind of injectivity index of each permeable bed. In addition, when the pore fluid temperatures of these permeable beds are different, change of flowrate at each permeable bed should cause temperature shift at permeable beds. Applying mass and energy balance, we can compute the pore fluid temperature except for the zone bearing the lowest pore fluid pressure. These three indexes, pore fluid temperature, pressure and injectivity are used to characterize permeable bed, which are useful for well-to-well correlation. Consequently those would serve to map and characterize permeable planes, which is useful for planning drilling target as well as production and re-injection management.

Although the number of wells logged is yet limited, the technique seems to render some remarkable results. For example, at least three major permeable planes were found in this particular reservoir section, which are positioned more or less in parallel. Only in such configuration, the pore fluids of adjacent permeable planes separated merely 50 meters or less in some area could exhibit temperature difference of more than 100 degrees Celsius.

INTRODUCTION

Hardware

Fiber optic sensor based on Raman back scattering is used to acquire instantaneous temperature profile over an entire wellbore up to the depth of 3,100 m. The logging system used is an advanced version of the one earlier developed by Watanabe et al.(1993) and Kitakoga et al.(1995). One of the main issues at that time was to suppress attenuation disturbances caused by hydrogen adsorption. The final product of their study withstood a downhole test under 170 degrees Celsius for three months without showing any noticeable degradation in the measured temperature data (Sumitomo Electric Industries (1995)).

The downhole measurement system consists of a single ended fiber housed in coaxial metal double tubes to allow nitrogen flushing. The above is then mechanically reinforced by armoring strands. The cable is designed to make it strong but flexible which is necessary feature for accommodating fragile and rigid optical fiber. The optical fiber used is a 50/125 GI coated by polyamide and silicone resin. The surface measurement instrument (SUT-110 of J-Power systems, Osaka Japan) adopts 850 nm diode laser. The temperature is derived by the ratio between

the Stokes and the anti-Stokes in order to reduce unwanted effects caused by transmission attenuation. In the following log data examples, the relationship between the Raman intensities and the temperature vs. the distance from the surface instrument. They clearly show that the anti-Stokes component is more sensitive to the temperature.

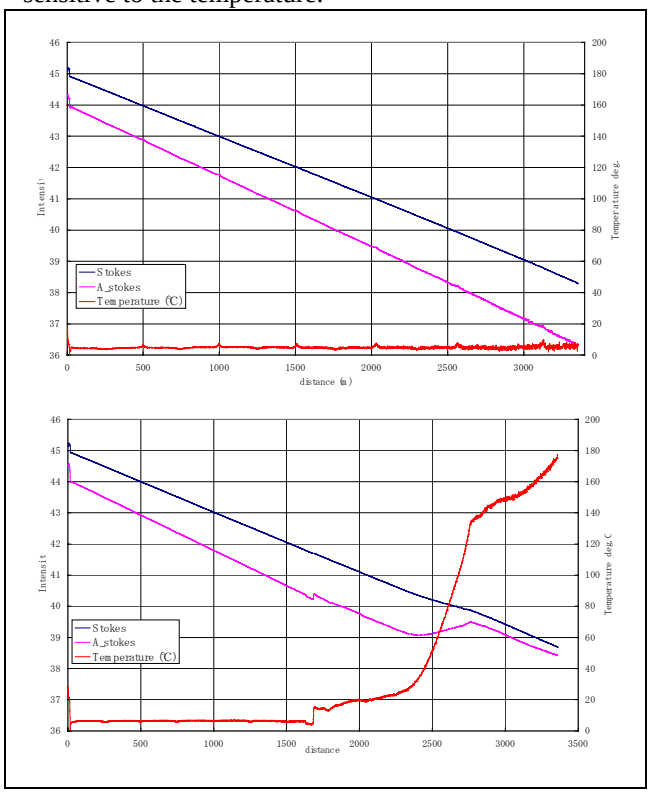

Figure 1. Examples showing the relationship between Stokes, anti-Stokes and temperature as to the distance from the surface instrument.

Measurement reliability

As mentioned above, the measurement reliability especially as to the disturbances caused by hydrogen adsorption has been one of the main issues for fiber-optic temperature measurement system to be established as a potentially viable well logging method. It happens to be that the basic feature of our system is also mentioned by Smithpeter et al.(1999) as possible solutions for this particular problem, though Normann at al.(2001) hinted that reducing hydrogen partial pressure may not prevent the degradation caused by hydrogen adsorption.

The temperature transformation for Raman scattering is related to the Bose-Einstein function.

$$\approx \frac{1}{\exp\left(\frac{hcv}{kt}\right) - 1}$$

Where h is Planck's constant, c is speed of light., v is Raman shift number, k is Boltzman constant and t is temperature. Because of the exponential nature as to temperature, measurement error in general gets progressively more evident at higher temperature. The simplest way to check cable quality is to make temperature measurement whilst placing the entire cable on the drum under ambient temperature. Degraded section may be noticeable as it is evidenced by anomalous temperature. However if the degradation is yet at minor degree, significant anomaly at elevated temperature may not be noticeable at ambient temperature level. Therefore it is preferable to check measurement accuracy at higher temperature. It is practically impossible to place an entire cable in an oven. An alternative method is to implement insitu temperature check in wells where their temperature profiles are stable. Thus we have conducted comparison measurements between the fiber optic temperature against the data taken by a conventional temperature log as an ultimate quality check.

In our case, the cable used for the study has so far gone through 18 runs of logging measurement under up to the maximum temperature of 286 degrees Celsius and the maximum depth of 2,290 m with accumulative hours in hole at 113 and accumulative traveling depth at 29 km. In between the above runs, comparisons were made on the fiber-optic temperature log and the temperature log taken from quartz memory gauges connected to the end of the fiber-optic cable. The discrepancy between the fiber optic temperature and the thermister temperature below the water level for both runs fell within the satisfactory range and showed negligible deterioration over the time.

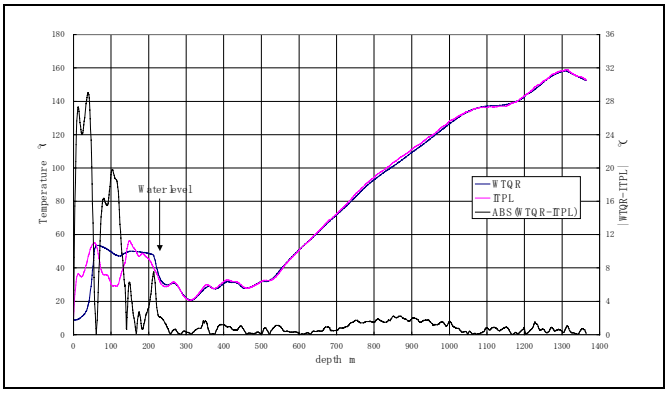

Figure 2. Comparison between the fiber optic temperature log data and the temperature data taken from quartz memory gauge.

Further quality check can be conducted at each logging run in the following manner. Because of uneven temperature exposure therefore uneven condition as to chemical reaction which the cable subject to, it is difficult to assume that the degradation due to hydrogen adsorption occurs evenly over a large interval of the cable. If a part of the cable (probably at the near end part of the cable) suffers the most from such degradation, the

phenomena can be easily detected by taking temperature measurement whilst placing the end of the cable at several different depths. In other words, if the temperature readings at a particular depth measured by different parts of the cable exhibit discrepancy bigger than the usual, one can assume the degradation may have occurred to the cable. Furthermore it should be possible to evaluate the extent of the damage by the amount of the anomaly at the given temperature level and the location of the cable. In the following figure, merged temperature profiles were obtained while the fiber optic temperature logging tool was stopped at every 100 meters. Meaningful anomaly is not recognized in this log example.

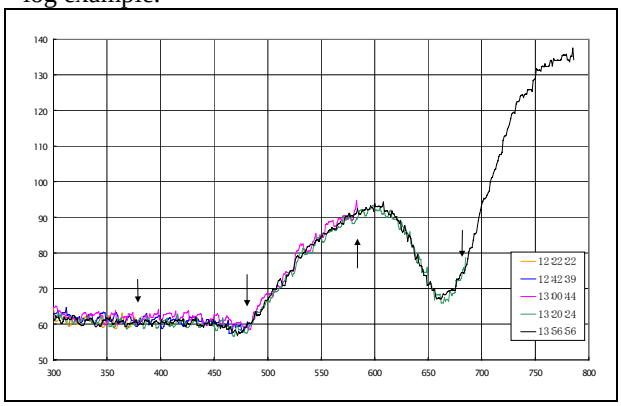

Figure 3. Examples of merged temperature profiles taken while the cable bottom at different depths.

Transient phenomena and flow profile log

The fiber optic distributed temperature log has several unique features as compared with the conventional temperature log. However it seems that attention has been mainly focused on utilizing it as convenient permanent temperature gauge while no particular interpretation techniques have been shown. Ikeda et al (2000) and Ikeda (2000) demonstrated the advantages and the potential applications of the instantaneous temperature profile acquisition. The papers described a way to derive fluid flow profile from successive temperature profiles during transient period in terms of temperature.

The following schematic illustration conveniently describes this particular interpretation technique. Fluid velocity profile is obtained, for example, while injecting water into highly permeable well. Water injected into a borehole pushes the fluid column downwards, thus it causes temperature profile to move at the same velocity as the fluid flow. Even for such a rapid temperature variation the fiber optic temperature log can easily capture the phenomena. The concept of this technique is similar to R/A tracer log. While R/A tracer log senses flow by the movement of R/A peak, flow profile delineated by the fiber optic log is by the movement of the unique temperature profile, which is acquired every 1 minute or so.

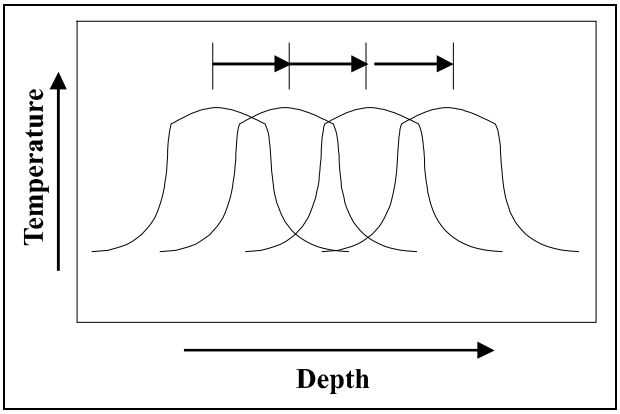

Figure 4. Schematic description of flow profile derivation from successive temperature recordings obtained by the fiber optic temperature log

An actual example is shown below where successive temperature profiles were acquired while injecting water into a well. It is clearly shown that the temperature profiles rapidly change up to the water level located just below 200m deep. Below that depth, they were shifted almost at regular intervals until at 300 m. Below that depth, the shifts become smaller but are kept almost constant until 400 m below which no more changes are seen on the profiles.

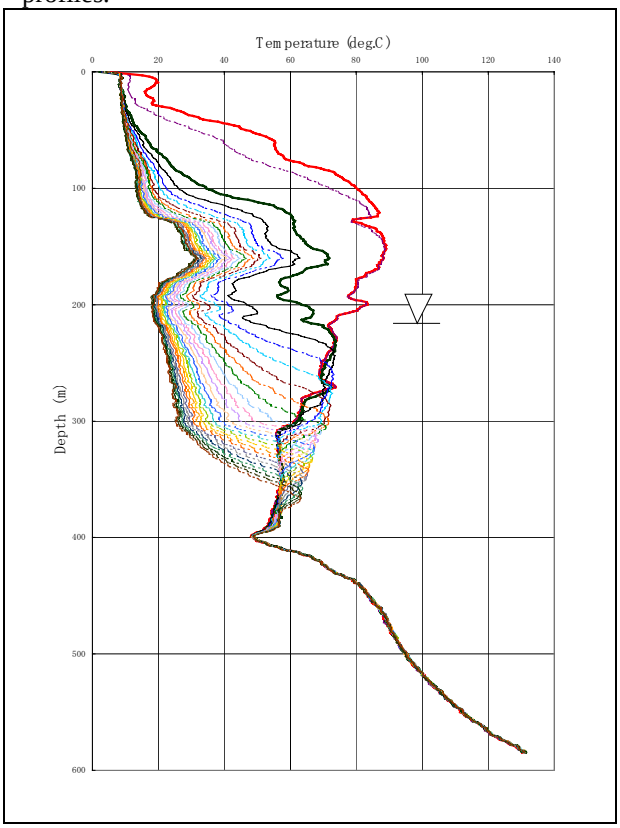

Figure 5. Fiber Optic Log acquired while injecting water.

In order to get a flow profile, curve correlation processing is applied to the above log example. It seems water injection was prematurely stopped as there should be flow up to 400 m deep according to the raw data.

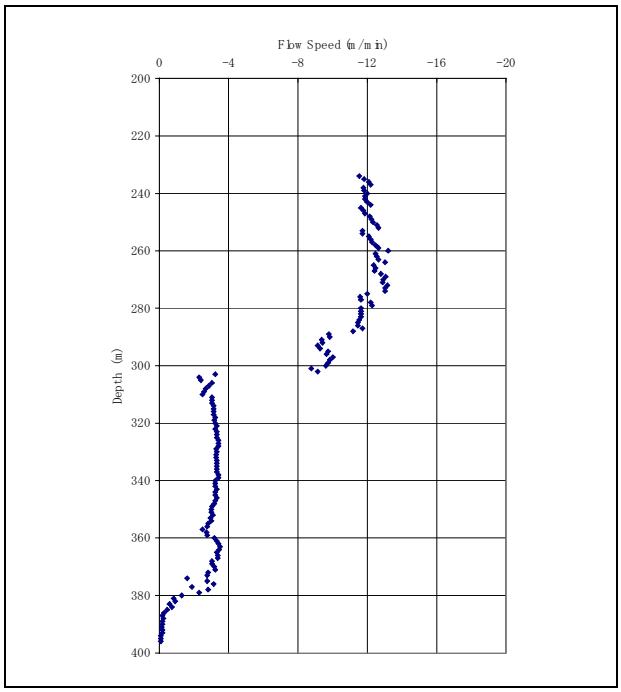

Figure 6. Flow profile derived from fiber optic temperature log.

Fluid flow to and out of fracture is usually seen for geothermal wells and even massive cross flows between permeable layers may occur. In a sense they may cause temperature disturbances. It however may be useful when coming to analyze physical property of fracture.

The temperature curves in the following figure were taken during a temperature recovery test. From these logging charts, one may notice that there are three distinctive temperature unconformities at the depth of 1,115m, 1,495m and 1,540m. Cross flows between these zones are attributed to these temperature unconformities. It also implies that these are the layers dominantly permeable in this well. It is however the best we could predict from the data which would be acquired by the conventional temperature logging.

If we can create transient temperature condition, the fiber optic distributed temperature log should be able to identify flow profile occurring in the well. Furthermore if the operation is properly manipulated, it is not only possible to predict details of the cross flow but also the pore pressure, the fluid temperature and qualitatively the injectivity index of each fracture zone though we have to bear in mind that these parameters obtained are limited to early transient state.

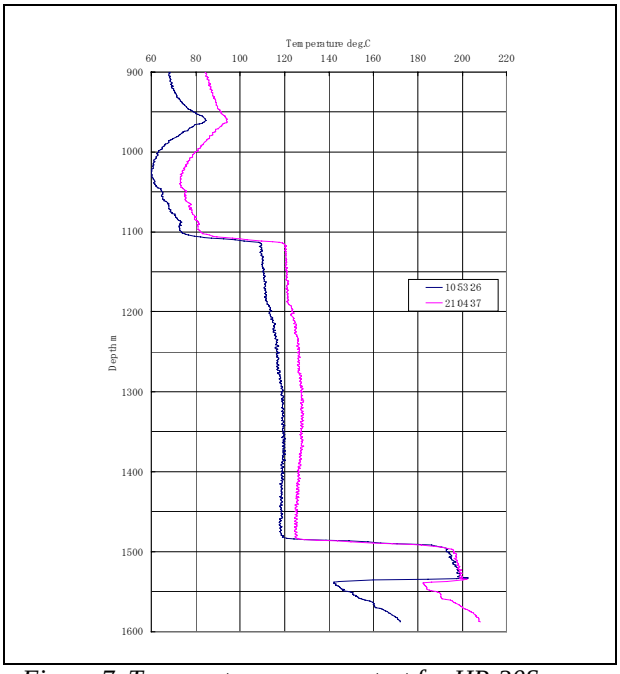

Figure 7. Temperature recovery test for HR-30S.

DISCUSSION

In order to analyze fluid flow profile during injection, at the end of temperature recovery test, fresh water is injected while observing temperature profile by the fiber optic distributed temperature as shown in fig.8. The successive temperature profiles were updated at every 65 seconds.

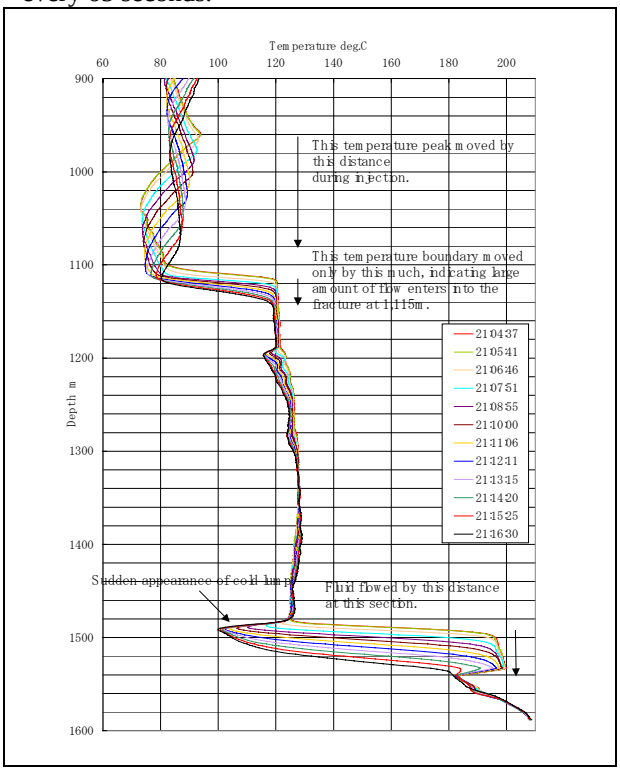

Figure 8. Temperature profiles during water injection for HR-30S.

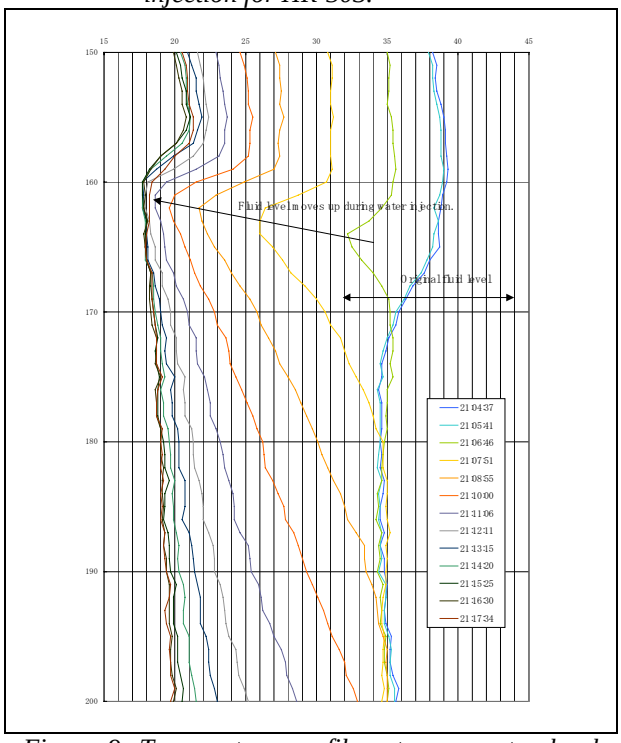

Figure 9. Temperature profiles at near water level during water injection for HR-30S.

The fluid level goes up and gets more or less stabilized at certain depth once water is injected as seen in fig.9. Meanwhile in fig.8, the temperature profiles are shifting gradually due to fluid flow. For example, the temperature peak originally located at 960m is moving at the converted flowrate similar to the one inside the casing. Thus it is predicted that injection flowrate is retained above 1,115m, implying there is no major fluid loss over this section. It however severely slows at 1,115m suggesting most of the fluid goes into the fracture at that depth.

What is more intriguing phenomena is a sudden appearance of apparently cold water lump at 1,495m, which slowly spreads downward until it reaches 1,540m. There seems no fluid movement below 1,540m. At this stage the cause of the cold water lump is not yet clear. However from the change of the temperature profiles a down-flow seems to be present all the way to 1,540m during injection. The flowrates at these three fractures are computed in the way explained above.

Once water injection stopped, the water level immediately returned to the original. It means the fluid flow(cross flows) also returned to the one present at the static condition. However since the temperature profile is distorted by water injection and no longer for the equilibrium state, we can then observe temperature profile change due to the cross flow occurring.

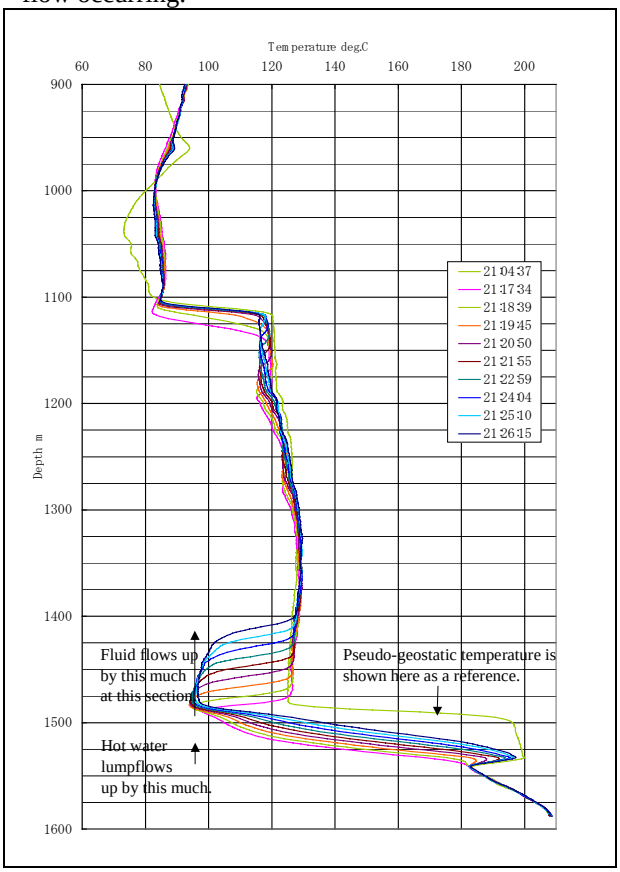

Figure 10. Temperature profiles after stooping water injection for HR-30S.

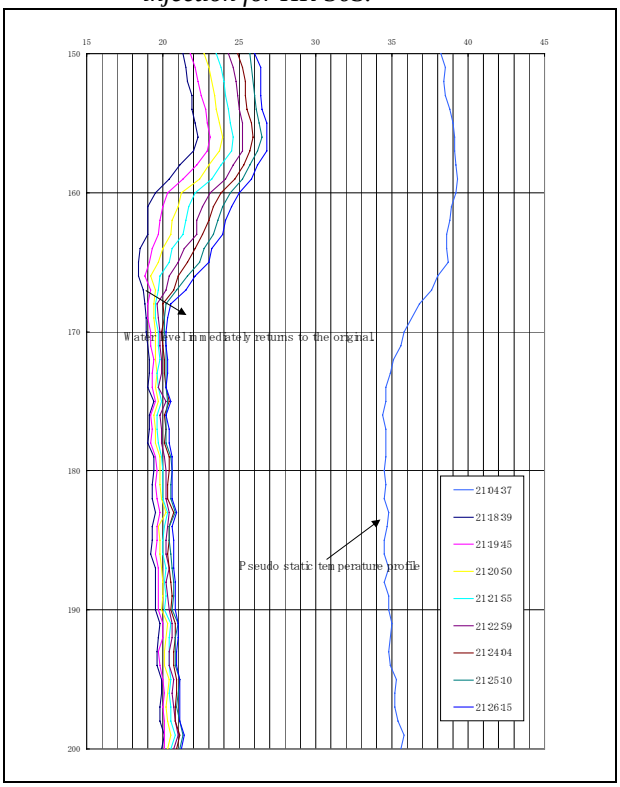

Figure 11. Temperature profiles at near water level after stooping water injection for HR-30S.

The fig. 10 clearly indicates that fluid at temperature of 204 degrees Celsius flows into the well at 1,540m and fluid at 94 degrees Celsius flows in at 1,495m. They are mixed and the resultant fluid has temperature of 124 degrees Celsius and flows up to 1,115m where it escapes into the fracture. In this way, the cross flows eventually make up the temperature profile seen at static condition in fig. 7.

By now we fully understand the state of the flow during the injection as follows. Most of the fluid injected escaped into the fracture at 1,115m while some went further below. The pore pressure at 1,495m was higher than the injection pressure so that it continued producing fluid with smaller rate. The pore pressure at 1,540m was less than the hydrostatic pressure during water injection. Thus the fluid coming down from above adds up to the fluid produced from 1,495m and further goes down till 1,540m where it escaped into the fracture. The flow conditions for both during the static and during the water injection is schematically shown in fig.12.

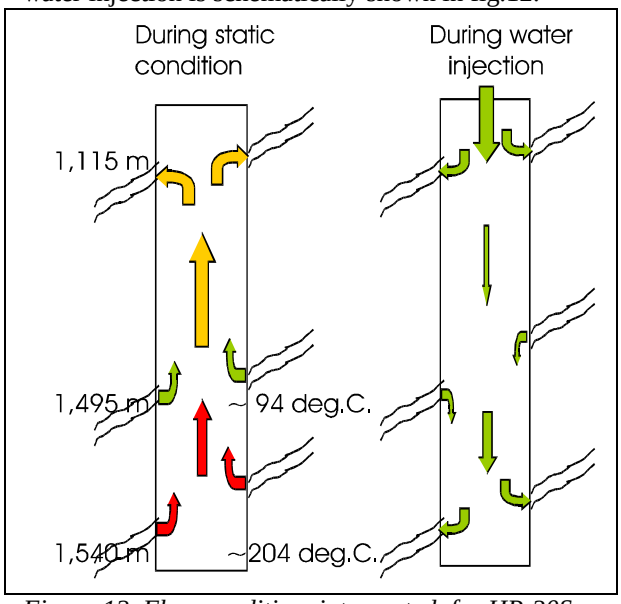

Figure 12. Flow condition interpreted for HR-30S.

For the two states of fluid flow, the hydrostatic pressure at each fracture depth can be computed by water level compensated for hole inclination and water density for temperature and compression. Since the temperature profile is constantly updated, the derived hydrostatic pressure should be reasonably reliable. As explained already, the flow occurring at each fracture for different hydrostatic conditions are computed by the fiber optic distributed temperature. Once these flowrates for the two different pressure conditions are found at each three fracture zones, it is possible to derive pore pressure and injectivity index of each fracture as shown in fig,13. Only remaining unknown is the fluid temperature at 1,115m, where the pore pressure is the lowest, hence no water is produced.

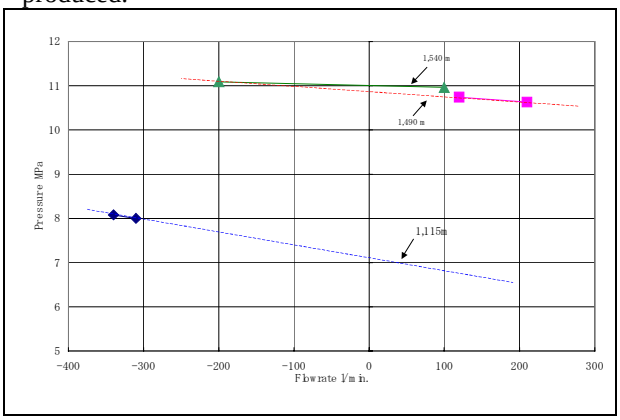

Figure 13. Flowrate vs. hydrostatic pressure for three fracture zones during static condition and during water injection at HR-30S.

	Water level			
Depth (TVD)	168 m at static condition		160 m during injection	
	Pressure Mpa	Flowrate l/min.	Pressure Mpa	Flowrate l/min.
1115 m (989.1 m)	8	-310	8.08	-340
1490 m (1276.3 m)	10.63	210	10.74	120
1540 m (1314.6 m)	10.96	100	11.09	-200

	Pore fluid pressure MPa	Pore fluid Temperature deg.C	Injectivity l/sec/MPa
1115 m (989.1 m)	7.17	N/A	~6
1490 m (1276.3 m)	10.82	~94	~14
1540 m (1314.6 m)	10.99	~204	~38

Table 1. Computed fracture properties.

If the physical properties of each fracture zone are identified, they will be very useful when correlating such zones over different wells. If such correlation is available for more than three wells, we can define fracture plane with high confidence. The advantage is obvious as it will give tremendous benefits in terms of planning future drilling, production or re-injection management. As we have seen in the above example, the fiber optic distributed temperature log could enhance well to well correlation for fracture when several fracture planes are crossing wells.

An attempt has been made to apply this interpretation technique to the re-injection section of the

Hacchobaru field. Since the data is acquired only when the new well is drilled, the number of wells logged is still limited. Furthermore, since all the well trajectories do not necessarily hit the same fracture planes, the study is not yet conclusive and still ongoing. Given such limitations, there are some interesting results I think worth presented.

So far we have been trying to correlate fracture planes based on the three main ones found in HR-30S and HR-28S, where those fracture planes are matched with high degree of confidence. The preliminary result is shown in the table 2. All the three planes appears running more or less in parallel. It may make sense if we look at the fact that in HR-30S, for example, there are fracture planes bearing pore fluid with temperature difference by about 110 degrees Celsius whilst being separated by merely 45 meters in the measured distance. We shall further enhance fiber optic temperature data in order to consolidate the findings and complete the subsurface mapping in respect to fracture planes the soonest.

		Dip (deg.)	Strike (deg)
Plane #1	No.1	54.7	-47.7
	No.2	53.8	-49.6
Plane #2	No.1	45.1	-63.8
	No.2	47.2	-63.3
	No.3	45.2	-63.3
Plane #3	No.1	50.5	-57.9
	No.2	54.7	-49.1

Table 2. Computed fracture plane direction. Each possible plane is computed by three points selected in wells. Strike is in reference to the true north.

Lastly I would like to draw your attention that all these benefits described are obtained through a sequential operation of the fiber optic distributed temperature log which is of course based on the temperature measurement, the most important measurement in geothermal well. Therefore this enhanced temperature measurement of the fiber optic distributed temperature does not require additional survey runs nor much more extra-time for the users of the conventional temperature survey.

CONCLUSION

A novel approach to delineate fractured reservoir using fiber optic temperature log is introduced. It is shown that the log has clear advantage in terms of transient wellbore phenomena associated with the temperature and successfully demonstrated the application of this logging technique which is not realized by the conventional temperature log. In certain way, it is one of the most powerful tool to delineate fractured type reservoir and has potential to open up a break through in this area of the study.

ACKNOWLEDGMENT

This development work is partly funded by the grant from Kitakyushu-City, Fukuoka-Pref., Japan. The author also would like to express sincere gratitude to Idemitsu Ooita Geothermal Co., Inc., Kyushu Electric Power Co., Inc. and NEDO for their assistance in the study as well as allowing to use their data.

REFERENCES

Ikeda, N., Uogata, K., Kawazoe, S., Haruguchi, K. (2000). "Delineation on Fracture Type Reservoir by Transient Temperature Monitoring using Fiber Optic Sensor," *Proceedings WGC2000*. C-2-3.

Ikeda, N., (2000). "Fractured Reservoir Management by Fiber Optic Distributed Temperature Measurement." *Proceedings SPWLA of Japan*.

Kawasaki, K. (2001), "Temperature Logging system using Fiber-Optic Sensor, Synopsis in Fiscal Year 2000 of Practical Examination of the Advanced Geothermal Technology Aimed at the Geothermal Development Cost Reduction." *Geothermal Energy(J. Geothermal Energy Development Center, New Energy Foundation, Japan)*, **96**, 4-23.

Kitakoga I., Oishi, K., Yasuhiro Ogata, Y., Masayoshi, Y., Nishima, H., Wada, O. and Nakura, Y. (1995). "Application of the fiber-optic distributed temperature sensor in geothermal wells." *Denkigakkai Electric Power/Energy Chapter*. 2pp.

Normann, R., Weiss, J. and Krumhans, J. (2000), "Development of fibers Optic Cables for Permanent Geothermal Wellbore development." *Proceedings, 26th workshop on geothermal reservoir engineering, Stanford University,* SGP-TR-168.

Smithpeter, C., Normann, R., Krumhans, J., Benoit, D. and Thompson, S. (1999). "Evaluation of a distributed fiber-optic temperature sensor for logging wellbore temperature at the Beowawe and Dixie Valley geothermal fields." *Proceedings, 24th workshop on geothermal reservoir engineering, Stanford University,* SGP-TR-162, 329-335.

Sumitomo Electeric Industries (1995). "Joint study report on Distributed Temperature Measurement System for Geothermal wells", *Internal Report*

Watanabe, K., Yasuga, H., Ogata, Y., Murata, Y., Nishida, H. and Wada O. (1993). "Fiber-Optic geothermal Wells Temperature Measurement System for Geothermal Power Plants." *Proceedings Denkigakkai Electric Power/Energy Chapter*. 2pp.